THE JOURNAL OF BIOLOGICAL CHEMISTRY
Vol. 277, No. 23, Issue of June 7, pp. 20919–20926, 2002

Printed in U.S.A.

Activation of Matrix Metalloproteinase-2 by Overexpression of Manganese Superoxide Dismutase in Human Breast Cancer MCF-7 Cells Involves Reactive Oxygen Species*

Received for publication, October 10, 2001, and in revised form, March 29, 2002
Published, JBC Papers in Press, April 2, 2002, DOI 10.1074/jbc.M109801200

Hannah J. Zhang‡, Weiling Zhao§, Sujatha Venkataraman§, Michael E. C. Robbins§, Garry R. Buettner§, Kevin C. Kregel‡, and Larry W. Oberley§¶

From the ‡Department of Exercise Science and §Free Radical and Radiation Biology Program, Department of Radiation Oncology, University of Iowa, Iowa City, Iowa 52242

Matrix metalloproteinases (MMPs) participate in cell migration and remodeling processes by affecting the extracellular matrix. MMP-2 is thought to be involved in cancer cell invasiveness. It has been proposed that the activity of MMP-2 can be modulated by intracellular reactive oxygen species (ROS)/reactive nitrogen species. We hypothesized that manganese superoxide dismutase (MnSOD) could mediate MMP-2 activity by changing the intracellular ROS level and that nitric oxide (·NO) may be involved in this process. Human breast cancer MCF-7 cells were stably transfected with plasmids containing MnSOD cDNA. A 2–30-fold increase of MnSOD protein and activity was observed in four clones. Our data demonstrated that overexpression of MnSOD stimulated the activation of MMP-2 with a corresponding elevation of ROS. A decrease in ROS by ebselen, a glutathione peroxidase mimetic, or by transduction of adenovirus containing human catalase or glutathione peroxidase cDNA abolished the effect of MnSOD on MMP-2 activation. Treatment of MCF-7 cells with antimycin A or rotenone increased intracellular ROS production and MMP-2 activation simultaneously. Our data also showed a suppression of endothelial nitric-oxide synthase expression that was accompanied by decreased ·NO production in MnSOD-overexpressing cells. However, the changes in endothelial nitric-oxide synthase and ·NO did not correlate with the MnSOD activity. Corresponding changes of MMP-2 activity after the addition of a NOS inhibitor (N^G-amino-L-arginine) or a ·NO donor ((*Z*)-1-[(2-aminoethyl)-*N*-(2-ammonioethyl)amino]diazen-1-ium-1,2-diolate) to the cells suggested the possibility that ·NO may be involved in the MnSOD-mediated MMP-2 activation pathway. These results indicate that MnSOD induces MMP-2 activity by regulation of intracellular ROS and imply that signaling pathways involving ·NO may also be involved in the MnSOD mediation of MMP-2 activity.

Cancer metastasis is a multistep process that includes invasion of cancer cells into blood vessels, traveling of these cells in the circulation system, and proliferation and eventual formation of a metastatic tumor at distal tissues. Among these steps, the first step of cancer cell invasion is a critical point for cancer metastasis. A current hypothesis proposes that remodeling of the extracellular matrix is a required process for cancer cell invasion (1, 2).

The process of extracellular matrix remodeling happens in both normal physiological conditions and pathological diseases such as cancer invasion. Cancer invasion is a disordered and uncontrolled behavior that usually involves the interaction of tumor cells and their surrounding stromal cells, leading to the loss of matrix function and a compromised matrix boundary. Although several classes of proteases have been suggested in extracellular matrix remodeling, previous studies have demonstrated that the activation of zinc-dependent matrix metalloproteinases (MMPs)[1] was the primary response for the degradation of components of the extracellular matrix (3, 4).

There are at least 15 members in the MMP family. MMP-2 (also called gelatinase A-type IV collagenase) and MMP-9 (geletinase B-type IV collagenase), two members of the MMP family, were postulated to play a critical role in tumor invasion. Lotta *et al.* have shown that the activities of MMP-2 and MMP-9 were higher in human breast cancer than the premalignant or normal breast tissue (1). In addition, in an experimental metastatic model, Stetler-Stevenson (5) has concluded that the protein level and activity of both enzymes were correlated with the metastatic potential of tumor cells.

MMPs share similar mechanisms of activation and protease function. The regulation of MMP activation occurs at both mRNA and/or protein levels. For example, transforming growth factor-β1 increases progelatinase mRNA levels in human fibroblasts (6). In addition, most MMPs are secreted as zymogens upon translation. Post-translational modification is required for MMP activation to acquire the proteolytic function.

Previously, oxidation and oxidative stress have been implicated in the regulation of MMP activation. Increases in MMP-2 mRNA level and enzymatic activity were seen following xanthine/xanthine oxidase (X/XO) treatment (7) and ionizing radiation (8). It is well known that both the X/XO system and radiation produce reactive oxygen species (ROS) such as superoxide radicals and hydrogen peroxide. In fact, hydrogen perox-

* This work was supported by NCI, National Institutes of Health (NIH), Grants P01 CA 66081 and CA84462, Public Health Service Grants AG 12350 and AG 14687, and NIDDK, NIH, Grant 51612. The costs of publication of this article were defrayed in part by the payment of page charges. This article must therefore be hereby marked "*advertisement*" in accordance with 18 U.S.C. Section 1734 solely to indicate this fact.

¶ To whom correspondence should be addressed: Free Radical and Radiation Biology, Dept. of Radiation Oncology, B180 ML, University of Iowa, Iowa City, IA 52242-1181. Tel.: 319-335-8015; Fax: 319-335-8039; E-mail: larry-oberley@uiowa.edu.

[1] The abbreviations used are: MMP, matrix metalloproteinase; ROS, reactive oxygen species; SOD, superoxide dismutase; DETA NONOate, (*Z*)-1-[(2-aminoethyl]-*N*-(2-ammonioethyl)amino]diazen-1-ium-1,2-diolate; CAT, catalase; GPx, glutathione peroxidase(s); TEMED, *N*,*N*,*N*′,*N*′-tetramethylethylenediamine; NBT, nitro blue tetrazolium; NOS, nitric-oxide synthase; eNOS, endothelial NOS; DFH, dihydrofluorescein; DA, diacetate; WT, wild type; MOI, multiplicity of infection.

ide has also been shown to increase the steady-state mRNA levels of collegenase/MMP-1 in human dermal fibroblasts (9). ROS are molecules that have higher reactivity than ground state dioxygen. ROS are constantly produced *in vivo* and cleared by cellular antioxidant systems. During normal physiological conditions, limited amounts of ROS may serve as signaling molecules in cell regulation pathways. However, an imbalance between production and removal of ROS can lead to oxidative stress due to the accumulation of these molecules. The consequences of intracellular oxidative stress include structural alterations of macromolecules, such as proteins causing enzymatic activation or inactivation, and disturbance in cellular signal transduction pathways that may stimulate or suppress gene expression.

The intrinsic antioxidant enzymes are essential for the protection of cells from oxidative stress. There are at least three families of primary antioxidant enzymes in mammalian cells. Superoxide dismutases (SODs) catalyze the conversion of superoxide to hydrogen peroxide, which is removed by catalase (CAT) or one of the glutathione peroxidases (GPx). Previously, manganese superoxide dismutase (MnSOD), a mitochondrial form of SOD, has been suggested as a tumor suppressor (10), and it is generally found at lower levels in tumors than in their normal cell counterparts (11, 12). Overexpression of MnSOD has been shown to suppress the tumor cell phenotype in several human cancer cell types (13–16). However, recent studies using immunohistochemistry have advanced our knowledge of the relationship of MnSOD and tumors. Several reports have shown that despite generally low levels of MnSOD in the center of solid tumor nests, there appeared to be very intense MnSOD staining in a few tumor cells located at the leading edge or outside layers of tumors adjacent to benign epithelium in breast and prostate tumors (17, 18). In addition, MnSOD expression is increased in metastatic gastric cancer (19). In a recent study, Lam *et al.* (20) found that overexpression of MnSOD by adenovirus gene transfer in hamster squamous carcinoma cells stimulated tumor cell invasive capacity as measured by the invasion chamber analysis. The fact that this elevation was abolished by adenovirus catalase suggested the involvement of ROS and particularly by hydrogen peroxide in the process of tumor invasion.

Therefore, we speculated that elevation of MnSOD without change of CAT and/or GPx would lead to the accumulation of peroxides and oxidative stress. The generated ROS and oxidative stress, in turn, could stimulate tumor invasiveness by an increase of MMP activation. The aim of this research was to the study of the effects of MnSOD on MMP-2 activation in human breast cancer MCF-7 cells. We hypothesized that MnSOD mediates MMP-2 activation by changing intracellular ROS levels. Furthermore, because nitric oxide (˙NO) is closely related to the ROS level by its direct reaction with superoxide, we further hypothesized that ˙NO may be involved in the regulation of MMP-2 activity by MnSOD.

Our results using MnSOD-overexpressing human breast cancer MCF-7 cells clearly demonstrated that MnSOD stimulated the activation of MMP-2. In addition, our data strongly suggested that ROS might be mediators for MMP-2 activation by MnSOD. Moreover, these data implied the possibility that ˙NO might also be involved in this pathway.

EXPERIMENTAL PROCEDURES

Materials—Nonessential amino acids and trypsin/EDTA were from the University of Iowa Cancer Center. Fetal bovine serum was from Hyclone Laboratories Inc. Eagle's minimum essential medium and Geneticin (G418) were from Life Technologies, Inc. Sodium pyruvate, rotenone, antimycin A, xanthine, xanthine oxidase, goat anti-rabbit IgG antibody conjugated with horseradish peroxidase, β-mercaptoethanol, bovine serum albumin, and TEMED were from Sigma. Nitro blue tetrazolium (NBT) was from Pierce. Riboflavin and the protein assay solution were from Bio-Rad. Nitrocellulose membranes were acquired from Schleicher & Schuell Co. Mouse antibodies against human nitric-oxide synthases (eNOS, inducible NOS, and neuronal NOS) were from Transduction Laboratories. The chemiluminescent ECL kit was from Amersham Biosciences. TiterMax Gold was from CytRX Co. Dihydrofluorescein diacetate (DFH-DA) was from Molecular Probes, Inc. (Eugene, OR). Ebselen was from Cayman Chemical Co. DETA NONOate and N^G-amino-L-arginine were from Alexis Co.

Cell Lines—Human breast MCF-7 cancer cells were stably transfected with control (Neo) vector or MnSOD cDNA. Two different forms of MnSOD cDNA were used to generate clones with different MnSOD activities as described in detail previously (15). Two different amino acids (either Ile or Thr) at position 58 of MnSOD resulted in two MnSOD proteins with different activities. The Ile form of MnSOD had 3 times the activity of the Thr form of MnSOD. The parental MCF-7 cells (WT), vector control cells (Neo), and four clones (SOD15, Mn52, Mn11, and Mn40) of MnSOD transfectants were routinely cultured in Eagle's minimum essential medium containing nonessential amino acids, 1 mM sodium pyruvate, and 10% fetal bovine serum. Media were changed every 3–4 days, and cells were incubated at 37 °C in a humidified atmosphere with 5% CO_2. G418 was constantly present in the media for Neo- and MnSOD-overexpressing cells at a concentration of 400 μg/ml. Five days before an analysis, cells were then placed in culture medium without G418 supplement.

Adenovirus Gene Transfer—Replication-defective recombinant adenovirus type 5 with the E1 region substituted with human CAT (Ad-CAT) or GPx (AdGPx) cDNA were provided by the Vector Core Facility of the University of Iowa. The infectious units of the adenovirus were typically at 1×10^{10} plaque-forming units/ml. Twenty-four h before adenovirus transduction, 5×10^6 or 5×10^3 cells were subcultured into a 60-mm dish or an eight-well chamber slide. At the time of infection, old media were replaced by fresh full media containing adenovirus at the designated multiplicity of infection (MOI). The cells were incubated with adenovirus for 24 h and then replaced by fresh media for an additional 24 h before being processed for assays. Control cells were treated by adenovirus containing empty vector (cytomegalovirus promoter only) (AdCMV) simultaneously with treatment groups.

Cell Treatment—Twenty-four h before a treatment, 5×10^6 or 5×10^3 cells were subcultured into a 60-mm dish or an eight-well chamber slide. At the time of treatment, old media were replaced by fresh full media containing chemicals at the designated concentration. Twenty-four h after a treatment, media were either changed again to full media without chemical supplements or processed for an assay immediately. For treatments with antimycin A and rotenone, control cells were incubated with media containing a similar concentration of vehicle solution (0.01% Me_2SO). In the situation where a ˙NO donor was used, a decomposed chemical solution was made by incubating the ˙NO donor solution at 37 °C for a period of at least 10 half-lives. Then it was added to the media in the same manner as the treatment group and served as control.

Protein Sample Preparation—The procedures for protein sample preparation were performed on ice. Cells were washed three times in cold phosphate-buffered saline and harvested by scraping and centrifugation. The cell pellets were resuspended in 50 mM potassium phosphate buffer (pH 7.8) and sonicated with four bursts of 30 s each using a Vibra Cell sonicator with a cup horn at full power. Total protein concentrations were determined by the Bradford assay using bovine γ–globulin as a standard.

Antibody Preparation—Pure human recombinant MnSOD protein was the kind gift from Dr. Joe McCord (University of Colorado). Rabbit anti–human MnSOD antibody was made in our laboratory. TiterMax Gold was used as adjuvant. One hundred fifty μg of MnSOD protein in 100 μl saline was mixed with 100 μl of the adjuvant and injected into the thigh of a female rabbit. After three boost injections, serum was collected and examined for MnSOD titer by Western blotting analysis. When a desired titer was reached, the rabbit was sacrificed, and serum was collected.

Western Blot Analysis—Equal amounts of total protein were analyzed by SDS-PAGE gel according to the method of Laemmli (21). The separated proteins were then transferred onto nitrocellulose membranes and blocked with 5% dry milk in Tris-buffered saline with 0.1% Tween 20 (TTBS). The nitrocellulose membranes were then incubated overnight at 4 °C with an antibody (1:1000) specific for the proteins of interest. After three washings with TTBS, the membranes were incubated with a secondary antibody conjugated with horseradish peroxidase (1:10,000) in TTBS for 1 h at room temperature. Blots were stained by the chemiluminescent ECL method, and immunoreactive signals

were visualized by exposure to a x-ray film.

MnSOD Activity Assay—SOD activity was measured by the modified NBT method described by Spitz and Oberley (22). This is an indirect assay based on a competition reaction between SOD and the superoxide indicator molecule, NBT. The rate of increase in the absorption at 560 nm over a 5-min time period indicates the reduction of NBT by superoxide. The competitive inhibition of this reaction is an indicator of total SOD activity. In the assay, the xanthine/xanthine oxidase system was used to generate superoxide. Varying amounts of total protein were added to the reaction until maximal inhibition was obtained as determined by spectrophotometry. Total SOD activity was determined by the amount of protein necessary for half-maximal inhibition of the NBT reaction. MnSOD activity was quantified in the presence of 5 mM NaCN, which only inhibits copper- and zinc-containing (CuZnSOD) activity. One unit of activity was defined as the concentration of SOD that reduced the NBT reaction to one-half of the maximum.

SOD, CAT, and GPx Activity Gel Assays—The native activity gel assay was used to measure the activity of SOD, CAT, and GPx. Total protein of each sample was separated in a native 8% polyacrylamide gel. For the SOD activity staining, as described by Beauchamp and Fridovich (23), the gel was incubated with 2.43 mM NBT, 28 μM riboflavin, and 28 mM TEMED for 20 min in the dark. After exposing the gel to a fluorescent light, the achromatic bands corresponding to SOD activity appeared on a dark blue background. For the CAT activity staining (24), the gel was first rinsed in distilled water three times and then incubated in 0.003% hydrogen peroxide for 10 min. The gel was then stained with 2% ferric chloride and 2% potassium ferricyanide. When achromatic bands demonstrating CAT activity appeared, the staining solution was replaced, and the gel was washed extensively with distilled water. The procedure for GPx activity staining was essentially the same as the CAT staining except that distilled water was replaced by 1 mM glutathione, and 0.008% cumene hydroperoxide was used as the substrate (24).

ROS Measurement—Intracellular ROS level was determined by measuring the oxidation of DFH-DA. DFH-DA is a nonpolar and nonfluorescent compound that can permeate cells freely. Once it is inside cells, the diacetate bond is cleaved by cellular esterases to form the polar and nonfluorescent DFH. Upon oxidation by ROS, this compound gives rise to DF that yields fluorescence. Five thousand cells were seeded 48 h prior the measurement and processed for treatments. At the time of the analysis, cells were washed three times with Hanks' buffer and then incubated with 500 μl of 5 μM DFH-DA solution for 15 min. After the incubation, cells were washed three times with Hanks' buffer and mounted with cover slides. Finally, the intensity of the fluorescence at 485/530 was recorded under a Bio-Rad MRC-600 laser-scanning confocal microscope.

MMP-2 Activity Assay—MMP-2 activity was measured by zymography. Zymography is a powerful electrophoretic technique for identifying proteolytic activity of enzymes separated in polyacrylamide gels under nonreducing conditions (25). To estimate the proteolytic activity of MMP-2, 1 mg/ml gelatin A was prepolymerized in a polyacrylamide gel as substrate. Proteins in 10 μl of conditioned serum-free medium were first separated electrophoretically at a constant voltage of 80 V for 2 h in the gel. After electrophoresis, the gel was washed in a buffer containing 2.5% Triton X-100 and 50 mM Tris-HCl (pH 8.0) for 2 × 30 min. The gel was then incubated overnight with a developing buffer containing 50 mM Tris, 10 mM $CaCl_2 \cdot 2H_2O$, 50 mM NaCl, and NaN_3 at 37 °C before it was stained with 0.25% Coomassie Blue in 25% isopropyl alcohol, 10% acetic acid for 30 min. The gel was destained in a destaining buffer with 10% methanol and 10% acetic acid until the wash remained clean and the achromatic bands appeared on the blue background. The gel was dried, scanned, and documented with an Epson Perfection 1200U scanner.

˙NO Measurement—A Sievers 280 nitric oxide analyzer was used to measure the amount of ˙NO produced by the cells. ˙NO once produced by cells in culture is quickly oxidized to nitrite. To measure this nitrite, the purge vessel contained a reducing agent (1% potassium iodine in glacial acetic acid) to convert nitrite to ˙NO. The ˙NO produced was swept into the nitric oxide analyzer, where it reacts with ozone, forming electronically excited nitrogen dioxide. The associated emission is proportional to the amount of ˙NO present in the sample. The amount of ˙NO made by the cells was determined by integrating the emission signal over time and was calibrated using known amounts of nitrite as a source of ˙NO.

The cells were rinsed with 5 ml of Hanks' buffer (37 °C). Then 3 ml of Hanks' buffer was added to the cells, and base-line nitric oxide production was determined. The cells were incubated for 3 h. After each hour, the amount of nitric oxide produced was measured. The levels of nitric oxide after 1, 2, and 3 h were used to determine the amount of ˙NO produced per hour. After all ˙NO measurements, the cells were scraped from the flasks and centrifuged. The cell pellets were resuspended in a phosphate buffer and stored at −80 °C for protein concentration estimation.

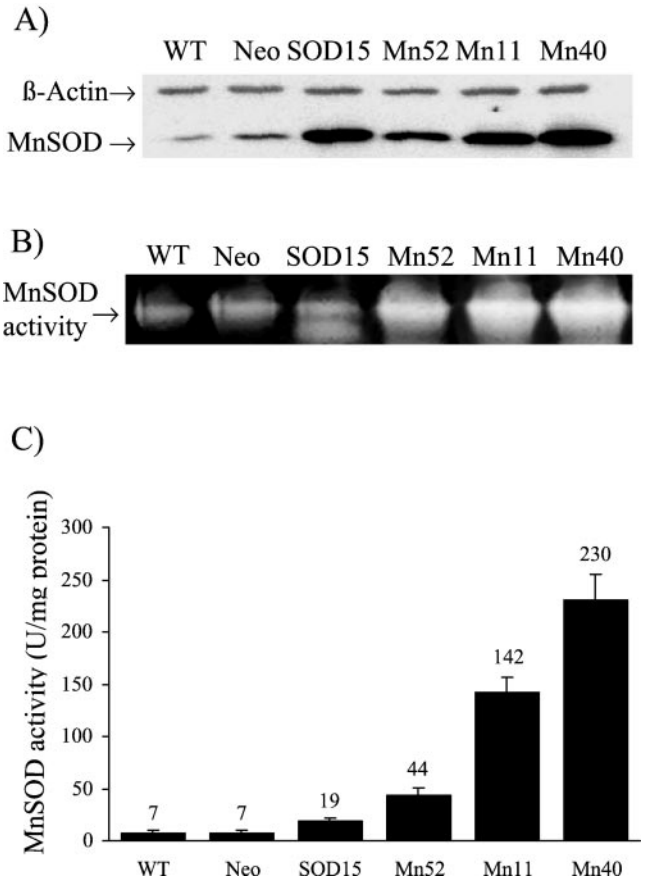

FIG. 1. **MnSOD is overexpressed in transfected human breast cancer MCF-7 cells.** *A*, MCF-7 cells were stably transfected by human MnSOD cDNA. Selected clones were examined by Western blotting analysis, which demonstrated an increase in immunoreactive protein levels in MnSOD-transfected cells. *B*, activity gel analysis showed different levels of elevation of MnSOD activity bands in MnSOD-overexpressing cells. *C*, SOD enzymatic activity measurement demonstrated increased MnSOD activities in MnSOD-overexpressing cells. One unit of activity was defined as the concentration of SOD that inhibits the NBT reduction rate to half of the maximum. Values at the *top* of each *column* represent mean MnSOD activity ± S.D. from four independent NBT assays shown in units/mg of protein. *, $p < 0.05$ compared with WT; *U*, units.

Statistical Analysis—Data are presented as means ± S.E. Analysis of variance-Tukey's multiple comparison was used to determine the statistical significance of the data at a level of $p \leq 0.05$.

Data Presentation—All of the data were from the average of at least three independent experiments. In the case of Western blotting, activity gels, and DFH staining, representative results that were repeated at least three times with similar results are shown.

RESULTS

Verification of MnSOD Overexpression—In this study, four MnSOD-overexpressing cell lines were used. These cell lines are SOD15, Mn52, Mn11, and Mn40. Their MnSOD expression along with those of WT and Neo vector control cells was verified previously (15). During this study, the levels of MnSOD in these cell lines were confirmed to ensure that there were no changes during cell culture (Fig. 1). Western analysis demonstrated increases in MnSOD protein levels in MnSOD overexpression cells when compared with WT and Neo cells (Fig. 1*A*). No changes were noted in β-actin expression, and it served as protein loading control. SOD15 was transfected with the Thr^{58}

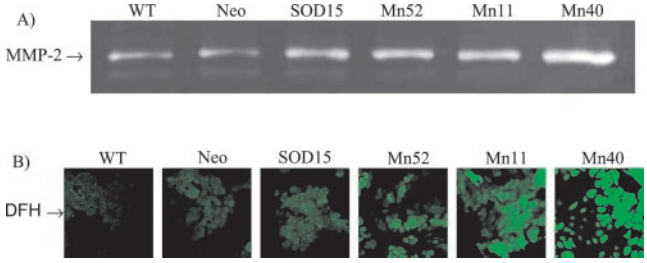

FIG. 2. **MnSOD overexpression stimulates MMP-2 activation and ROS accumulation in a dose-dependent manner.** *A*, 10 μl of conditioned serum-free medium were first separated electrophoretically in a 10% nondenaturing polyacrylamide gel containing 1 mg/ml gelatin A as substrate. Then the gel was incubated for the enzyme digestion reaction and stained by Coomassie Blue. The gel was destained in a destaining buffer until the achromatic bands representing the activity of MMP-2 appeared on a dark blue background. *B*, 5000 cells were seeded and measured for ROS level by incubating with 5 μM DFH-DA for 15 min. The intensity of the fluorescence representing the oxidation of DFH by ROS was examined at 485/530 nm by confocal laser scanning microscopy. Experiments were repeated at least three times with similar results. Representative results are shown.

form of MnSOD cDNA, which yielded a large increase in MnSOD protein but only a small elevation in activity level (Fig. 1, *B* and *C*). This observation was consistent with our previous report (15). Mn52, Mn11, and Mn40 were transfected with the Ile^{58} form of MnSOD and showed 6-, 19-, and 30-fold increases in MnSOD activity, respectively. The activities of CuZnSOD, CAT, and GPx were also measured. No significant changes were noted among all cell lines (data not shown).

MnSOD Induces MMP-2 Activation and Increases ROS Levels—To study the effects of MnSOD on MMP-2 activation, MCF-7 cells overexpressing MnSOD were assayed for MMP-2 activation by zymography. Fig. 2*A* shows that MMP-2 activity was elevated as the MnSOD levels increased. The brightest band, representing the highest MMP-2 activity, was seen in Mn40 cells that had the highest MnSOD activity. Correspondingly, the levels of intracellular ROS in these cells were also elevated, with the Mn40 cell line being the highest as measured by DFH fluorescent staining (Fig. 2*B*).

ROS Mediate the Activation of MMP-2 by MnSOD—To test the causal effect of ROS on the activation of MMP-2 by MnSOD, different concentrations of ebselen, a GPx mimic, were used to treat Mn40 cells. ROS levels and MMP-2 activity were measured after the treatment. A decrease in DFH fluorescence was observed in a dose-dependent manner (Fig. 3*A*, *i*). At an ebselen concentration of 50 μM, a marked reduction of DFH fluorescence was detected. Moreover, at a concentration of 100 μM, complete inhibition was seen. Zymographic analysis of the conditioned media from the same cells demonstrated dramatic reduction in MMP-2 activity after 50 and 100 μM ebselen treatment (Fig. 3*A*, *ii*), which is directly related to the suppression of ROS in these cells. Cell viability was measured after ebselen treatment by the 3-(4,5-dimethylthiazol-2-yl)-2,5-diphenyltetrazolium bromide assay, and cell death was not observed (data not shown).

Because ebselen has also been shown to scavenge other oxidants, specifically peroxynitrite, more specific approaches were used. Recombinant adenovirus containing human CAT or GPx cDNA were applied to Mn40 cells at 0, 5, 10, 25, and 50 MOI. The activities of CAT and GPx along with ROS levels and the activation of MMP-2 were examined after the transduction. As shown in Fig. 3*B*, Mn40 cells, which have a low level of endogenous CAT activity, exhibit increased levels of CAT activity after AdCAT transduction (Fig. 3*B*, *i*). Accompanying the increases in CAT activity, a moderate decrease of DFH staining (Fig 3*B*, *ii*) and a clear suppression of MMP-2 activity (Fig. 3*B*, *iii*) were observed. AdGPx was also transduced into Mn40 cells to study the role of ROS in MMP-2 activation. Fig. 3*C* demonstrates the results from the AdGPx transduction. Mn40 cells, which had undetectable endogenous GPx activity, clearly had dose-dependent increases in GPx activity, with the highest activity after 50 MOI AdGPx transduction (Fig. 3*C*, *i*). Conversely, the DFH fluorescence was decreased in a dose-dependent manner and to a very low level after 50 MOI AdGPx transduction (Fig. 3*C*, *ii*). More dramatically, the suppression of MMP-2 activation was evidenced after application of as little as 10 MOI AdGPx and was dose-dependent in correlation with the DFH fluorescence (Fig. 3*C*, *iii*).

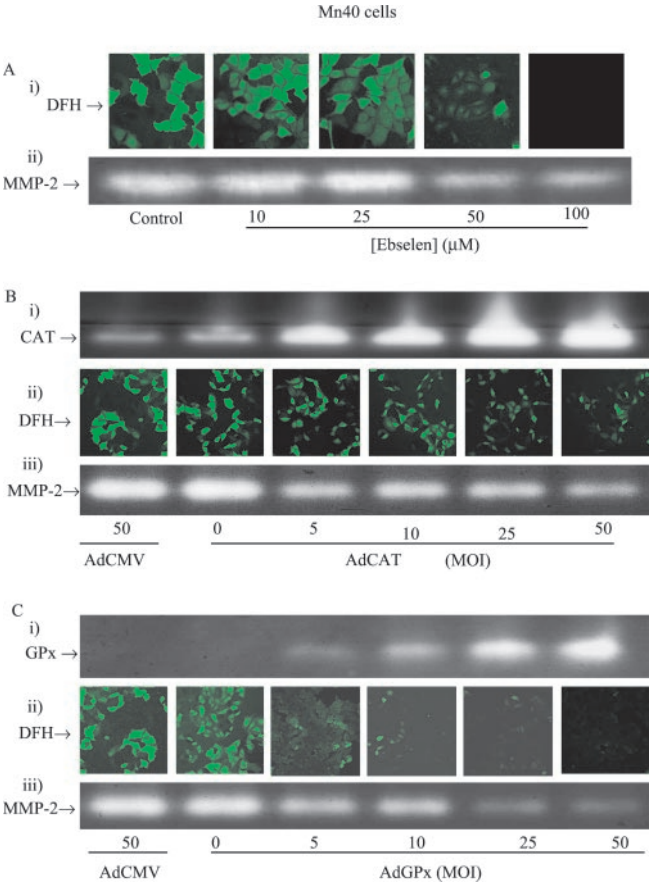

FIG. 3. **Ebselen treatment and adenovirus CAT and GPx decreased the ROS accumulation and MMP-2 activation in MnSOD-overexpressing cells.** *A*, *i*, 5000 Mn40 cells were plated for 24 h and then treated with the designated concentrations of ebselen for another 24 h. ROS levels were measured as described in the legend to Fig. 2*B*. *ii*, 10 μl of conditioned media from ebselen-treated cells were measured for MMP-2 activity as described in the legend to Fig. 2*A*. *B* and *C*, 5000 Mn40 cells were plated for 24 h and then transduced with designated MOI of adenovirus. CAT (*B*, *i*) and GPx (*C*, *i*) activities were measured by activity gel assay. *ii*, ROS levels were measured as described in the legend to Fig. 2*B*. *iii*, MMP-2 activity was measured as in Fig. 2*A*. Experiments were repeated at least three times with similar results. Representative data are shown.

To further demonstrate that ROS stimulate the activation of MMP-2, MCF-7 WT and Neo cells were incubated with either antimycin A or rotenone. Both antimycin A and rotenone are cellular electron transport chain inhibitors that increase electron leakage from the electron transport chain, leading to an increase in intracellular ROS (26, 27). Cell survival was first measured by the 3-(4,5-dimethylthiazol-2-yl)-2,5-diphenyltetrazolium bromide assay after treatment (Fig. 4*A*). At a concentration of 10 μM, 95% of the cells treated with antimycin A had normal function with no significant difference between WT and Neo. Meanwhile, 90% of cells treated with rotenone survived

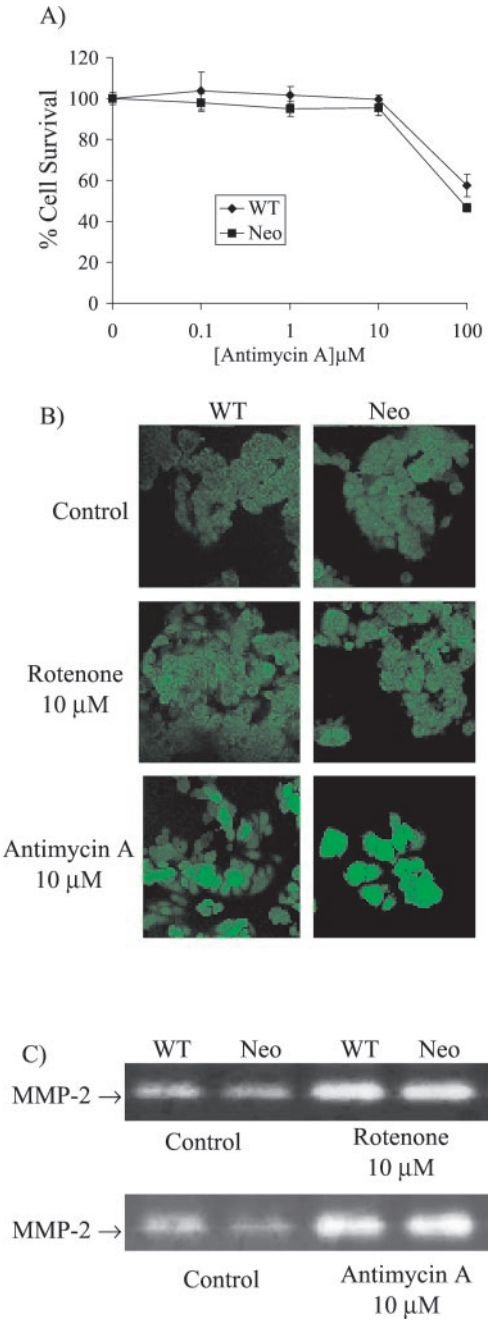

FIG. 4. **Antimycin A and rotenone treatments induced ROS accumulation and MMP-2 activation.** *A*, 5000 WT and Neo cells were seeded in a 96-well plate 24 h before antimycin A treatment. The cells were then treated with the designated concentrations of antimycin A. Twenty-four h after treatment, cell survival was measured by the 3-(4,5-dimethylthiazol-2-yl)-2,5-diphenyltetrazolium bromide assay. Mean cell survival ± S.D. from at least three independent 3-(4,5-dimethylthiazol-2-yl)-2,5-diphenyltetrazolium bromide assays is shown. Rotenone treatment was processed in a similar protocol (data not shown). B, 5000 WT and Neo cells were treated as described for *A*. ROS levels were measured as described in the legend to Fig. 2*B*. *C*, 10 μl of conditioned media from antimycin A- and rotenone-treated cells were measured for MMP-2 activity as described in the legend to Fig. 2*A*. Experiments were repeated at least three times with similar results. Representative images are shown.

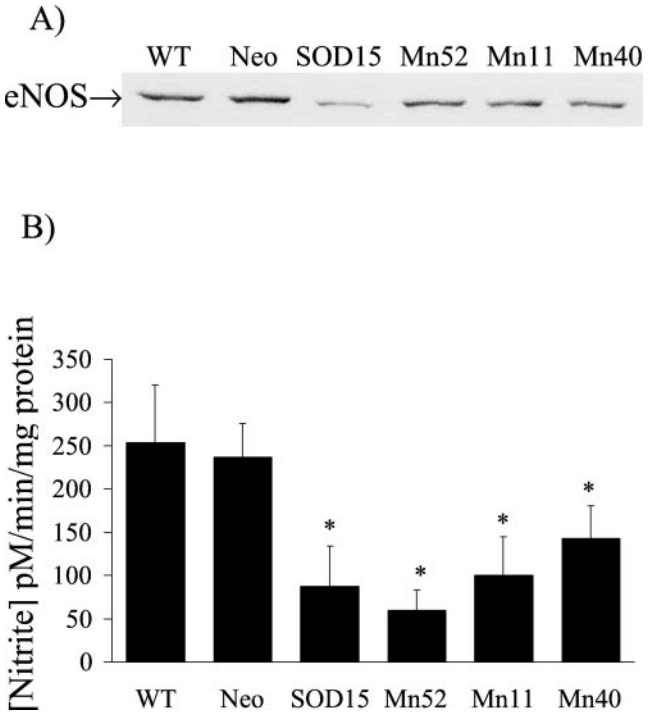

FIG. 5. **MnSOD overexpression suppressed eNOS expression and lowered ·NO production.** *A*, 30 μg of total protein was separated on a 5–20% gradient SDS-PAGE gel and blotted for eNOS expression. The membrane was stained by the ECL method. The experiment was repeated three times with similar results. A representative result is shown. *B*, 80% confluent cells were used for ·NO measurements by a Sievers 280 nitric oxide analyzer. Three ml of Hanks' buffer were added to the cells and base-line ·NO production was determined. The cells were incubated for 3 h, and after each hour the amount of ·NO produced was measured to determine whether the amount of nitric oxide produced was linear with time. The levels of ·NO after 1, 2, and 3 h were used to determine the amount of ·NO produced per hour. The amount of ·NO produced was normalized to the protein concentration of each cell line. Each column represents mean nitrite concentration ± S.D. from three independent experiments. *, $p < 0.05$ compared with WT.

with no significant difference between the two cell lines (data not shown). Therefore, the levels of DFH staining and MMP-2 activity in WT and Neo cells were measured after 10 μM antimycin A or rotenone treatments. A dramatic increase in DFH fluorescence was observed (Fig. 4*B*). This increase correlates with a significant induction of MMP-2 activation (Fig. 4*H*). Rotenone also increased DFH fluorescence and MMP-2 activation but to a lesser extent when compared with the untreated control cells (Fig. 4, *B* and *C*).

·NO May Be Involved in the Regulation of MMP-2 Activation by MnSOD—Because ·NO can directly react with superoxide to form peroxynitrite, we postulated that ·NO might play a role in the modulation of MMP-2 activation by MnSOD. Intracellular NOSs were first examined by Western blotting analysis on cells overexpressing MnSOD. The levels of endothelial NOS were reduced in MnSOD-overexpressing cells when compared with WT and Neo cells (Fig. 5*A*). Inducible and neuronal NOS were not detectable by Western blotting in all of the cells (data not shown). The production of ·NO was also estimated by using a Sievers 280 nitric oxide analyzer. ·NO production was significantly decreased in MnSOD overexpressing cells (Fig. 5*B*). This observation is consistent with the Western analysis of NOS. However, the dose responses that were seen in MMP-2 activation were not noted in ·NO production. SOD15 and Mn52, the two cell lines with moderate increases in MnSOD levels, had the most inhibition of ·NO production. Mn11 and Mn40, which had very high MnSOD expression, had statistically significant but moderate reduction of ·NO production.

To further examine whether ·NO has effects on MMP-2 activation, N^G-amino-L-arginine (500 μM), a NOS inhibitor, was used to treat cells (Fig. 6*A*). In addition, Mn15 cells, with the lowest levels of eNOS and nitrite production among the Mn-SOD overexpression cell lines, were treated with different concentrations of DETA NONOate, a ·NO donor (Fig. 6*B*). Results

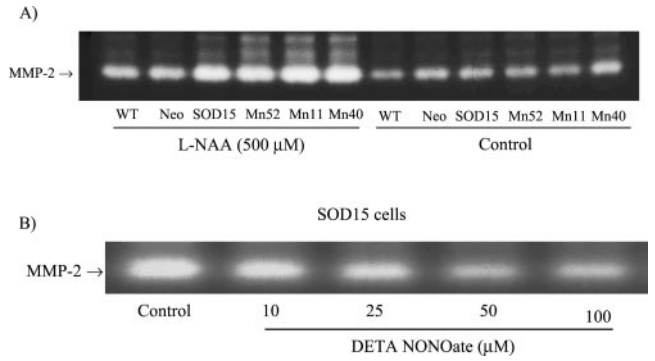

FIG. 6. **MMP-2 activation was increased by a NOS inhibitor and suppressed by a ·NO donor.** Five million cells were seeded 24 h before N^G-amino-L-arginine (*L-NAA*; *A*) or DETA NONOate treatments (*B*) at the designated concentration. Twenty-four h after the treatments, 10 μl of conditional media were used to measure MMP-2 activity as described in the legend to Fig. 2*A*. Experiments were repeated at least three times with similar results. Representative images are shown.

from these experiments suggested that the NOS inhibitor increased the activation of MMP-2 in all cells at 500 μM concentration, whereas the ·NO donor decreased the activity of MMP-2 in SOD15 cells even at 10 μM concentration.

DISCUSSION

A previous study has indicated that MnSOD might promote the invasiveness of tumors (20). The aim of the present research was to examine whether MnSOD could up-regulate the activation of MMP-2, a major enzyme involved in extracellular matrix remodeling in the tumor invasion process. Furthermore, because ROS/reactive nitrogen species have been implicated in the stimulation of MMP-2 expression (7–9), we also investigated whether ROS/reactive nitrogen species might be the mediator in the activation of MMP-2 by MnSOD in breast cancer cells. To determine this, human breast cancer MCF-7 cells were stably transfected with two forms of human MnSOD cDNA. Four MnSOD-overexpressing cell lines selected from the transfection had different levels of MnSOD activities ranging from 3- to 30-fold increases over the wild type MCF-7 cells or those transfected with the vector *neo* gene. Analysis of MMP-2 activity in these cell lines clearly demonstrated that overexpression of MnSOD increased the MMP-2 activity. Moreover, it was evident that this induction of MMP-2 activity was in a dose-dependent manner such that it was correlated with the enzymatic activities of MnSOD rather than their protein levels. SOD15 cells have a mutated form of MnSOD that gives rise to a 9-fold increase of MnSOD protein but only a 3-fold increase in enzyme activity. These cells had only a small induction of MMP-2 activity. Meanwhile, Mn11 and Mn40 cells had substantial increases in MnSOD activity to levels that may not be seen in normal physiological conditions. The MMP-2 activation was greatly induced in these two cell lines. This observation correlates with other reports that MnSOD levels are unusually high in metastatic tumors (19) or are higher at the invasive edge of solid tumors compared with the center of the tumor or the surrounding normal tissues (17, 18). This indicates that MMP-2 may be one of the important players in the effects of MnSOD on tumor metastasis. Presumably, MnSOD stimulates the activation of MMP-2 that in turn increases tumor cell invasiveness.

Because MnSOD is an enzyme that catalyzes the conversion of superoxide to hydrogen peroxide, an accumulation of hydrogen peroxide or other peroxides can happen without proper peroxide removal mechanisms in MnSOD-overexpressing cells. Others have demonstrated that an imbalance between peroxide accumulation and removal could lead to an increase in ROS levels and oxidative stress (28–31). In the present study, the activities of CAT and GPx, two enzymes that are critical to peroxide removal, did not change with MnSOD overexpression. Measurements of ROS levels by DFH-DA fluorescent staining demonstrated an accumulation of ROS after MnSOD overexpression. It is noteworthy that the extent of MMP-2 activation correlated with the extent of ROS accumulation. These data suggest a strong linkage between ROS accumulation and MMP-2 activation in MnSOD-overexpressing cells.

DFH-DA freely diffuses through cell membranes. Once it enters the cells, its ester moiety is cleaved by intracellular esterases, and then DFH is retained in the cells. Oxidation of DFH by ROS yields a fluorescent species that can be detected by confocal microscopy. Although there is uncertainty over the specific oxidants that oxidize DFH in cells, it has been well documented that DFH is an important tool to indicate oxidations in cells and is one of a very few markers available for measuring intracellular ROS levels in live cells (32–35)

To determine whether ROS, specifically peroxides, are involved in the pathway of MnSOD up-regulation of MMP-2, Mn40 cells, the cells with highest MMP-2 activity, were treated with ebselen, a well established synthetic selenium-containing compound with GPx mimetic properties (36, 37). This treatment dramatically suppressed DFH fluorescence at concentrations of 50 and 100 μM. Correspondingly, a marked suppression of MMP-2 activation was also seen with these two dosages.

To more specifically pinpoint peroxide involvement, Mn40 cells were further transduced with recombinant adenovirus containing CAT or GPx cDNA. Dose-dependent increases in both CAT and GPx activities were clearly seen after adenovirus transduction. Not surprisingly, ROS levels and MMP-2 activation were decreased, corresponding to CAT and GPx levels. Interestingly, GPx had larger effects on the decline of ROS levels and suppression of MMP-2 activation than CAT. Two possibilities may account for this phenomenon. First, because GPx reacts with H_2O_2, lipid peroxides, and/or peroxynitrite, whereas CAT removes only H_2O_2, the larger effect of GPx may indicate the participation of lipid peroxides and/or peroxynitrite in the activation of MMP-2. Our results from the treatment of ebselen, which also removes both H_2O_2 and peroxynitrite, support this possibility. Second, the subcellular location of GPx may play a role. GPx is primarily located in the cytosol. There is evidence of its presence also in mitochondria (38), where MnSOD resides. Catalase is primarily in peroxisomes, which is some distance away from MnSOD. Thus, both location and the nature of the peroxides/peroxynitrite will be the subject of future studies. Nevertheless, our results strongly suggest that peroxide and/or peroxynitrite levels increase with MnSOD overexpression, and they establish a clear, causal relationship between ROS and MMP-2 activation.

There is controversy over whether peroxides (especially hydrogen peroxide) levels are elevated upon SOD overexpression. Some believe that the production of ROS (hydrogen peroxide) does not change with changing SOD levels and that only the rate of dismutation of superoxide is affected by SOD because peroxide production is a function of how much superoxide is produced, not how fast it is dismutated. Our results indicate that peroxide levels do increase with MnSOD overexpression. In addition, three additional observations support our results: 1) catalase or glutathione peroxidase levels increase in response to SOD overexpression in some cell lines (11, 13); 2) DFH fluorescence increases after SOD overexpression in our cells and other cells (30); and 3) overexpression of either glutathione peroxidase (30) or catalase (39) inhibits the tumor-suppressive effect of MnSOD overexpression. Moreover, we

have been working on a kinetic model to explain why hydrogen peroxide levels increase after MnSOD overexpression. This model shows that, because of Le Chatelier's principle, the removal of superoxide by SOD can result in some superoxide-producing reactions to actually make more superoxide (*e.g.* coenzyme Q making more superoxide (40)). This additional superoxide can be dismuted by SOD to produce more hydrogen peroxide.

Tools other than MnSOD manipulation were also used to stimulate ROS production and MMP-2 activation. WT and Neo cells were treated with two mitochondrial electron transport chain inhibitors, antimycin A and rotenone. Antimycin A inhibits the function of complex III, while rotenone inhibits the function of complex I of the mitochondrial electron transport chain. Previous reports have shown that by inhibition of the electron transport chain, these two chemicals induce the production of superoxide (26, 27). Presumably, the superoxide produced can be converted to peroxide by spontaneous dismutation or by SOD. The DFH fluorescent staining results showed a moderate increase after rotenone treatment and a strong induction after antimycin A treatment, suggesting an elevation of peroxide levels. The MMP-2 activation was also observed and correlated with peroxide production in these treatments. These observations provide direct evidence that ROS increase MMP-2 activity.

Our results are consistent with those of Wenk *et al.* (41). This group has studied the effect of MnSOD overexpression on the induction of the interstitial collagenase MMP-1 in human skin fibroblasts. They showed via Northern blotting that oxidants like UVA irradiation and paraquat increased MMP-1 mRNA levels in MnSOD-transfected cells compared with controls. They proposed that hydrogen peroxide was the inducing agent, because agents that increased hydrogen peroxide levels in the cells by inhibiting peroxide removal (3-amino-1,2,4-triazole to inhibit catalase and buthionine sulfoximine to inhibit glutathione synthesis) strongly increased MMP-1 mRNA levels even without the presence of exogenous oxidizing agents.

Overall, our data strongly support the hypothesis that ROS are involved in the modulation of MMP-2 activation by MnSOD. The mechanisms on how ROS regulate MMP-2 activation are not clear and warrant future investigations. Much evidence has indicated that accumulation of ROS leads to the alteration in a wide range of gene expression, such as antioxidant enzymes, stress response genes, and cytokines (reviewed in Ref. 42). Previously, reports have also shown that radiation and xanthine/xanthine oxidase treatments induced the mRNA expression of MMP-2 (7, 8), indicating an up-regulation of MMP-2 gene expression by ROS. Moreover, it has been proposed that a post-translational regulation of MMP-2 activation may be also involved in the ROS regulation pathway via a "cysteine switch" mechanism (43). A cysteine in the highly conserved amino-terminal (activation locus) (PRCG*X*PDV) region of MMP-2, which serves as a pro fragment peptide, is required in maintenance of MMP latency. This unpaired cysteine residue is a critical residue that usually directly coordinates with the zinc atom at the active site. Disruption of the interaction between the zinc atom and this unpaired cysteine initiates a cascade of reactions that lead to final activation of MMPs. Deletion of this cysteine residue has led to the autoactivation of MMPs (43, 44). On the other hand, the synthetic peptides (PRCG*X*PDV) inhibited not only the activation of MMPs (45–47) but also neoplastic cell invasion (48).

In general, the intracellular peroxide level is kept in a delicate balance between production and clearance. Evidence from others has established that nitric oxide can react directly with superoxide to form peroxynitrite (49). This reaction may compete with MnSOD for superoxide and thus may affect the production of peroxides. We examined the levels of nitric oxide in MnSOD-overexpressing cells and found that ·NO production was decreased in these cells. The reduction of ·NO is probably due to the decrease in eNOS expression, since Western blotting analysis showed a reduction of eNOS protein level with MnSOD overexpression but not inducible or neuronal NOS. The reason for eNOS suppression by MnSOD overexpression is unknown at this point. The observation that NOS inhibition results in increases of MMP-2 activation and that a ·NO donor partially depresses the activation of MMP-2 implies the possibility of the involvement of ·NO in the regulation of MMP-2 activity. However, unlike MnSOD overexpression, a direct dose response was not observed for MMP-2 activation with ·NO production. These data suggest that ·NO might be indirectly involved in the regulation of MMP-2 activation.

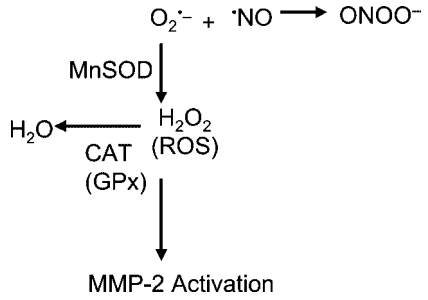

FIG. 7. **Possible regulation pathway for MMP-2 activation by MnSOD.**

In conclusion, as indicated in Fig. 7, our study demonstrates a pathway by which MnSOD regulates the activation of MMP-2 in tumor cells. Our results clearly suggest that a balance between the production and the removal of ROS, especially peroxides, plays an important role in the MMP-2 activation. MnSOD and other antioxidants that affect the levels of intracellular ROS can have a direct influence on MMP-2 activation. These data also suggest that signaling pathways involving ·NO may participate in the MnSOD mediation of MMP-2 activity.

Acknowledgments—We acknowledge the Central Microscopy Research and Learning Facility at the University of Iowa for the technical assistance in use of the confocal microscope. We thank the Vector Core Facility of the University of Iowa for providing adenovirus.

REFERENCES

1. Lotta, L. A. (1984) *Am. J. Pathol.* **117,** 339–348
2. Stetler-Stevenson, W. G., Aznavoorian, S., and Liotta, L. A. (1993) *Annu. Rev. Cell Biol.* **9,** 541–573
3. Birkedal-Hansen, H., Moore, W. G. I., Bodden, M. K., Windsor, L. J., Birkedal-Hansen, B., DeCarlo, A., and Engler, J. A. (1993) *Crit. Rev. Oral Biol. Med.* **4,** 197–250
4. Crawford, H. C., and Matrisian, L. M. (1994) *Invasion Metastasis* **14,** 234–245
5. Stetler-Stevenson, W. G. (1990) *Cancer Metastasis Rev.* **9,** 289–303
6. Overall, C. M., Wrana, J. L., and Sodek, J. (1991) *J. Biol. Chem.* **266,** 14064–14071
7. Siwik, D. A., Pagano, P. J., and Colucci, W. S. (2001) *Am. J. Physiol.* **280,** C53–C60
8. Zhao, W., O'Malley, Y. Q., Wei, S., and Robbins, M. E. C. (2000) *Int. J. Radiat. Biol.* **76,** 391–402
9. Brenneisen, P., Briviba, K., Wlaschek, M., Wenk, J., and Scharffetter-Kochanek, K. (1997) *Free Radic. Biol. Med.* **22,** 515–524
10. Bravard, A., Sabatier, L., Hoffschir, F., Ricoul, M., Luccioni, C., and Dutrillaux, B. (1992) *Int. J. Cancer* **51,** 476–480
11. Oberley, L. W., and Buettner, G. R. (1979) *Cancer Res.* **39,** 1141–1149
12. Oberley, L. W., and Oberley, T. D. (1986) in *Free Radicals, Aging, and Degenerative Diseases* (Johnson, J. E. J., Walford, R., Harmon, D., and Miquel, J., eds) pp. 352–377, Alan R. Liss, New York
13. Liu, R., Oberley, T. D., and Oberley, L. W. (1997) *Human Gene Ther.* **8,** 585–595
14. Yan, T., Oberley, L. W., Zhong, W., and St. Clair, D. K. (1996) *Cancer Res.* **56,** 2864–2871
15. Zhang, H. J., Yan, T., Oberley, T. D., and Oberley, L. W. (1999) *Cancer Res.* **59,** 6276–6283
16. Zhong, W., Oberley, L. W., Oberley, T. D., and St. Clair, D. K. (1997) *Oncogene* **14,** 481–490

17. Thomas, P. A., Oykutlu, D., Pou, B., Tyler, D., Oberley, L. W., Robinson, R. A., and Lenel, J. C. (1997) *Pathol. Oncol. Res.* **3,** 278–286
18. Bostwick, D. G., Alexander, E. E., Singh, R., Shan, A., Qian, J., Santella, R. M., Oberley, L. W., Yan, T., Zhong, W., Jiang, X., and Oberley, T. D. (2000) *Cancer Metastasis Rev.* **89,** 123–134
19. Malafa, M., Margenthaler, J., Webb, B., Neitzel, L., and Christophersen, M. (2000) *J. Surg. Res.* **88,** 130–134
20. Lam, E. W., Zwacka, R., Seftor, E. A., Nieva, D. R., Davidson, B. L., Engelhardt, J. E., Hendrix, M. J., and Oberley, L. W. (1999) *Free Radic. Biol. Med.* **27,** 572–579
21. Laemmli, U. K. (1970) *Nature* **227,** 680–685
22. Spitz, D. R., and Oberley, L. W. (1989) *Anal. Biochem.* **179,** 8–18
23. Beauchamp, C., and Fridovich, I. (1971) *Anal. Biochem.* **44,** 276–287
24. Sun, Y., Elwell, J. H., Oberley, L. W. (1988) *Free Radic. Res. Commun.* **5,** 67–75
25. Seftor, R. E. B. (1994) *Electrophoresis* **15,** 454–462
26. Paradies, G., Petrosillo, G., Pistolese, M., and Ruggiero, F. M. (2000) *FEBS Lett.* **466,** 323–326
27. Vanden Hoek, T. L., Shao, Z., Li, C., Schumacker, P. T., and Becker, L. B. (1997) *J. Mol. Cell Cardiol.* **29,** 2441–2450
28. Amstad, P., Peskin, A., Sha, G., Mirault, M. E., Moret, R., Zbinden, I., and Cerutti, P. (1991) *Biochemistry* **30,** 9305–9313
29. Amstad, P., Moret, R., and Cerutti, P. (1994) *J. Biol. Chem.* **269,** 1606–1609
30. Li, S., Yan, T., Yang, J.-Q., Oberley, T. D., and Oberley, L. W. (2000) *Cancer Res.* **60,** 3927–3939
31. Zhong, W., Oberley, L. W., Oberley, T. D., Yan, T., Domann, F. E., and St. Clair, D. K. (1996) *Cell Growth Differ.* **7,** 1175–1186
32. Bass, D. A., Parce, J. W., Dechatelet, L. R., Szejda, P., Seeds, M. C., and Thomas, M. (1983) *J. Immunol.* **130,** 1910–1917
33. Carter, W. O., Narayanan, P. K., and Robinson, J. P. (1994) *J. Leukocyte Biol.* **55,** 253–258
34. Hempel, S. L., Buettner, G. R., O'Malley, Y. Q., Wessels, D. A., and Flaherty, D. M. (1999) *Free Radic. Biol. Med.* **27,** 146–159
35. Royall, J. A., and Ischiropoulos, H. (1993) *Arch. Biochem. Biophys.* **302,** 348–355
36. Maiorino, M., Roveri, A., and Coassin, M. (1988) *Biochem. Pharmacol.* **37,** 2267–2271
37. Parham, M. J., and Graf, E. (1987) *Biochem. Pharmacol.* **36,** 3095–3102
38. Esworthy, R. S., Ho, Y. S., and Chu, F. F. (1997) *Arch. Biochem. Biophys.* **340,** 59–63
39. Rodriguez, A. M., Carrico, P. M., Mazurkiewicz, J. E., and Melendez, J. A. (2000) *Free Radic. Biol. Med.* **29,** 801–813
40. Schafer, F. Q., and Buettner, G. R. (2001) *Free Radic. Biol. Med.* **30,** 1191–1212
41. Wenk, J., Brenneisen, P., Wlaschek, M., Poswig, A., Briviba, K., Oberley, T. D., and Scharffetter-Kochanek, K. (1999) *J. Biol. Chem.* **274,** 25869–25876
42. Camhi, S., Lee, P., and Choi, A. M. (1995) *New Horizons* **3,** 170–182
43. Park, A. J., Matrisian, L. M., Kells, A. F., Pearson, R., Yuan, Z. Y., and Navre, M. (1991) *J. Biol. Chem.* **266,** 1584–1590
44. Sanchex-Lopex, R., Nicholson, R., Gesnel, M.-C., Matrisian, L. M., and Breathnach, R. (1988) *J. Biol. Chem.* **263,** 11892–11899
45. Nomura, K., and Suzuki, N. (1993) *FEBS Lett.* **321,** 84–88
46. Stetler-Stevenson, W. G., Talano, J. A., Gallagher, M. E., Krutzsch, H. C., and Liotta, L. A. (1991) *Am. J. Med. Sci.* **302,** 163–170
47. Van Wart, H., and Birkedal–Hansen, H. (1990) *Proc. Natl. Acad. Sci. U. S. A.* **87,** 5578–5582
48. Melchiori, A., Albini, A., Ray, J. M., and Stetler-Stevenson, W. G. (1992) *Cancer Res.* **52,** 2353–2356
49. Beckman, J. S., Beckman, T. W., Chen, J., Marshall, P. A., and Freeman, B. A. (1990) *Proc. Natl. Acad. Sci. U. S. A.* **87,** 1620–1624